Research Square

Preprints are preliminary reports that have not undergone peer review.
They should not be considered conclusive, used to inform clinical practice,
or referenced by the media as validated information.

# Estimating Total Precipitable Water Using Atmospheric Thermodynamic and Aerosol Parameters Associated with Thunderstorms

**Imad Abdulridha Al-Khulaifawi**

imadjasim900@gmail.com

Southern Federal University, Institute of Earth Sciences

**Aqeel Ghazi Mutar**

Mustansiriyah University

**Research Article**

**Keywords:** Thunderstorms, Particulate matter PM2.5, Total precipitable water, Cloud top temperature, CAPE, Integrated water vapor transport

**Posted Date:** October 8th, 2026

**DOI:** https://doi.org/10.21203/rs.3.rs-10930739/v1

**License:** This work is licensed under a Creative Commons Attribution 4.0 International License.
Read Full License

**Additional Declarations:** No competing interests reported.

# Estimating Total Precipitable Water Using Atmospheric Thermodynamic and Aerosol Parameters Associated with Thunderstorms

**[1]Imad Abdulridha Jasim Al-Khulaifawi**

**[2]Aqeel Ghazi Mutar**

imadjasim900@gmail.com

[1]Department of Oceanology, Institute of Earth Sciences, Southern Federal University, Rostov-on-Don, Russian Federation.

[2]Department of Atmospheric Sciences, College of Science, Mustansiriyah University, Baghdad, Iraq.

**Abstract**

This study provides a comprehensive physical and statistical assessment of the dynamic cross-impact interaction between particulate matter (PM2.5) and atmospheric thermodynamic coefficients during thunderstorm-formation cycles in Iraq. This study analyzes thunderstorm activity based on archival data from meteorological observations and satellite data (NCEP/NCAR and MERRA-2) over 16 years at Baghdad, Basra, Mosul, and Sulaymaniyah Airport Stations. The analysis showed that the highest frequency of thunderstorms occurs in April, reaching (29, 41, 21, and 57), respectively. The best particulate matter concentration of 2.5 at Mosul Airport Station before, during, and after the storm (B) was moderate (the analysis was proven by the multiple linear regression equation in Figure 13), and the worst particulate matter concentration was at Basra Airport Station (D), which was unhealthy, and this is a dangerous indicator: the concentration continued to rise without addressing the causes. Burning natural gas and oil is a well-known source of pollutants that pollute Iraq's air. The results of evaluating the associations between TPW and atmospheric parameters using a Pearson correlation model showed that TPW concentrations were positively correlated with particulate matter (PM2.5), convective available potential energy (CAPE), and integrated water vapor transport (IVT) but negatively correlated with cloud top temperature (CCT). Statistical verification showed high efficiency and stability of the proposed model (multiple linear regression for $TPW_{Est}$) with a correlation coefficient (R) ranging between (0.70 and 0.77), making it a promising tool to support digital extreme weather forecasting and air quality management in different environments.

**Keywords:** Thunderstorms, Particulate matter PM2.5, Total precipitable water, Cloud top temperature, CAPE, Integrated water vapor transport.

## 1. Introduction

A thunderstorm is a convective storm that typically forms in cumulonimbus clouds. It produces thunder and lightning. A thunderstorm is likely to form when cold, dry air in the atmosphere covers warm, humid surface air. This makes the atmosphere conditionally unstable. There are three stages in a thunderstorm's life cycle. During the forming stage, cumulus clouds expand as rising air currents (updrafts) occur, producing sporadic lightning and little to no precipitation. Next, the storm enters its mature stage. This stage features simultaneous updrafts and downdrafts while precipitation falls. This results in gust fronts and often severe weather, including hail, strong winds, heavy rain, lightning, and occasionally tornadoes. Ultimately, downdrafts stifle updrafts during the dispersing stage, causing a sharp drop in storm strength and extensive precipitation (Brázdil et al., 2020; Kolendowicz et al., 2017; Krider, 2021; Pekárová et al., 2021; Púčik et al., 2013; Roy et al., 2023; Stull, 2017; Taszarek et al., 2020). Single-cell, multicellular, and supercell storms are the three main categories of storms. Three primary factors influence the generation of thunderstorms: (a) unstable air, (b) lifting action, and (c) the atmospheric moisture content (Arora et al., 2023; Bennett et al., 2006; Kunz et al., 2020; Stull, 2017; Trapp, 2013). Additionally, the vertical movement of water droplets above the freezing point is made easier by increased convective available potential energy (CAPE) from urban heat, which improves charge separation and flash formation (Steiger & Orville, 2003). Moist convection is a complex process that

makes a significant contribution to the determination of the atmospheric thermodynamic state, particularly in the tropics. The convective available potential energy (CAPE) is commonly used for assessing the potential for deep moist convection in the atmosphere. This quantity actually serves as a measure of moist-convective instability of the atmosphere (Augstein et al., 1974; Emanuel, 1994).

Total precipitable water is a crucial metric for quantifying the water vapor content, representing the cumulative volume of water vapor in the atmospheric column that can condense and precipitate as rain or snow. PM2.5 is predominantly concentrated in the lower atmosphere and significantly influences the precipitation process, thereby affecting the characteristics of precipitation (Wang et al., 2025). The local evolution of PW is therefore determined by evaporation (E), precipitation (P), and a factor representing the convergence of moisture fluxes integrated vertically. Evaporation enhances precipitable water (PW), whereas precipitation diminishes PW, serving as the catalyst for deep convection. PW simulation algorithms and models provide more stable and less ambiguous predictive interpretations than direct estimations of surface rainfall variables, resulting in exceptional reliability for mathematical models, evidenced by a correlation coefficient exceeding 0.98 in monitoring frontal weather disturbances (Misva, 2021). Other experts claim that the rotational part of the moisture flux carries moisture from two main areas: the Indian Ocean, Arabian Sea, Gulf of Aden, the Red Sea, and the Atlantic and Mediterranean Seas (Abdeldym et al., 2019).

One of the main causes of air pollution is particulate matter (PM). The city's PM concentration and distribution are influenced by a number of elements, including local weather patterns, including wind direction and speed; temperature; relative humidity; and rainfall, all of which can help to maintain low pollution levels (Galindo et al., 2011). According to a study, the degree to which aerosols and atmospheric thermodynamics are intertwined remains unclear, despite extensive examination of their interactions at various scales. Since more atmospheric instability is needed to overcome the greater aerosol levels, there is evidence that lightning activity in urban thunderstorms is sensitive to both thermodynamic conditions and aerosol concentrations. Therefore, lightning output appears to be enhanced in situations where there are both large concentrations of aerosols and high levels of atmospheric instability, which is frequently the case in urban areas (Bentley et al., 2024; Sun et al., 2023). Moreover, natural factors are no longer the only driver of these storms; research on the interplay between the atmosphere and human activities has shown that aerosols emitted markedly increase lightning intensity, thereby deepening our comprehension of cumulus cloud dynamics in a contaminated setting (Asfur et al., 2023).

The rise in total column mass PM2.5 correlates with a decline in cloud-top temperature; this relationship appears unexplained unless the cloud-top temperature is considered a function of cloud-top height. The elevation of cloud tops can be attributed to enhanced condensation processes within the clouds due to the rise in organic carbon levels. This process will emit more energy as latent heat, rendering the air parcels highly unstable, thus allowing buoyancy to reach its maximum altitude and hence augmenting the depth of the clouds (Mutar, 2024). The gaseous state known as water vapor is important to the physical and chemical processes that occur in the atmosphere, playing a role in the size and composition of hygroscopic aerosol particles and affecting the optical properties of aerosols. Furthermore, atmospheric water vapor is vital for the formation of clouds and rain, as it can remove dissolved gases and aerosols from the atmosphere (Sirikaew et al., 2025).

Several studies in the literature have analyzed the relationship between thunderstorms, total precipitation water, and particulate matter (PM2.5). The researchers (Al-Khulaifawi & Ioshpa, 2026) analyzed the relationship between thunderstorm activity and air pollutant concentrations (PM2.5) at Baghdad Airport and Basra Airport international stations over a period of twenty years (2000-2019). The methodology was based on combining ground-based observational data with reanalysis data from ERA-5 and MERRA-2. The study recorded that the highest frequency of thunderstorms occurs during the spring, specifically in April, at a rate of 64.03%. The results showed that the concentrations of PM2.5 at the two stations before, during, and after the storms fell within category (D) according to air quality indicators (concentrations ranging between 55.5 and 150.4 $\mu g/m^3$), indicating a continuously polluted environment. The study concluded that there is a direct correlation between dry thunderstorms and increased pollutants, PM2.5, which calls for the development of weather forecasting models that consider the impact of

convective phenomena on air quality in semi-arid regions. (Sae-Jung et al., 2025) This study analyzes the relationship between thermodynamics, aerosols, and thunderstorms in Bangkok, utilizing lightning strike counts as an intensity metric during a five-year span (2016–2020). The project utilizes data from the Aerosol Robotic Network (AERONET), ERA-5 reanalysis, terrestrial air quality stations, and total lightning data from Vaisala Inc.'s GLD360 network to analyze the interrelationships between aerosols and thermodynamics in conditions conducive to thunderstorm initiation. The results demonstrate that aerosol effects on thunderstorms are significant and, when analyzed alongside instability, can enhance lightning activity. Thermodynamic instability is positively associated with stroke counts in thunderstorms. A study (Wang et al., 2025) examined and estimated particle concentrations (PM2.5) in southern China by employing cumulative machine learning algorithms and models. The methodology was based on the integration and analysis of precipitation water vapor (PWV) data from global satellite navigation systems (GNSS), data (radiosonde), and pollution monitoring stations. The results revealed a close correlation and solid physical correlation between changes in the vertical water content of the atmosphere and the rates of accumulation and dispersion of particle pollutants, as the developed cumulative model proved highly efficient and accurate in simulating and predicting aerosol concentrations under various surrounding climatic conditions. The study also revealed that the highest and lowest levels of PM2.5 concentrations were closely related to terrain and population factors. The Sirikaew et al. (2025) study developed an artificial neural network (ANN) model to estimate monthly rates of total precipitable water (TPW) content in Thailand, based on long-term surface meteorological data spanning from 2008 to 2024. The methodology relied on integrating surface temperature coefficients, relative humidity, and saturated water vapor pressure deduced from the developed Magnus formula. Although there were weak to moderate correlations between the independent variables and TPW, the developed ANN model demonstrated superior predictive ability and very high statistical reliability in the testing phase, where the coefficient of determination ($R^2$) recorded advanced values ranging between (0.81 and 0.98) with an average radical error rate (RMSE) that did not exceed 4.83% across different stations.

Despite growing global studies investigating the mechanisms of interaction between atmospheric and aerosol physics, the nature of the dynamic and thermal relationship between micro-air pollutants (PM2.5) and total precipitation (TPW) water content during thunderstorm development remains unclear, especially in humid, dry, and semi-arid environments such as the Middle East. In addition, climate studies in Iraq suffer from a clear gap in integrating and matching real-time ground-based observational data with international 3D reanalysis models (NCEP/NCAR and MERRA-2) to build estimated mathematical models that combine surface pollutants and hydrodynamic coefficients to explain the behavior of wet and dry thunderstorms. This study mainly aims to explore and analyze the weather patterns of thunderstorms and the physical correlation relationship between TPW (total precipitation water) and thermodynamic coefficients (convective available potential energy (CAPE), integrated water vapor transport (IVT), cloud top temperature (CCT), and particulate matter (PM2.5)) in Iraq across four major airport stations (Baghdad, Basra, Mosul, and Sulaymaniyah) for an extended period of 16 years (2010–2025). The study also seeks to develop an innovative mathematical equation based on the multiple linear regression model for calculating estimated water content ($TPW_{Est}$) and verify its efficiency to support digital prediction of weather disturbances and their environmental impacts.

## 2. Materials and Methods

### 2.1. Study Area

Iraq is located in western Asia, northwest of the Arabian Peninsula, between 29°5′ and 37°22′ N latitude and 38°45′ and 48°45′ E longitude. The country consists of four primary physiographic regions, each characterized by distinct climates: the alluvial plain and desert plateau with a hot desert climate, the mountainous range with a Mediterranean climate, and the steppe-terrain region with a semi-arid climate. The elevation and location of these regions significantly influence the climatic conditions across Iraq (Al-Ansari, 2021; Al-Khulaifawi & Ioshpa, 2025). Figure 1 presents the topography of Iraq and the locations of the selected Baghdad, Basra, Mosul, and Sulaymaniyah Airport Stations.

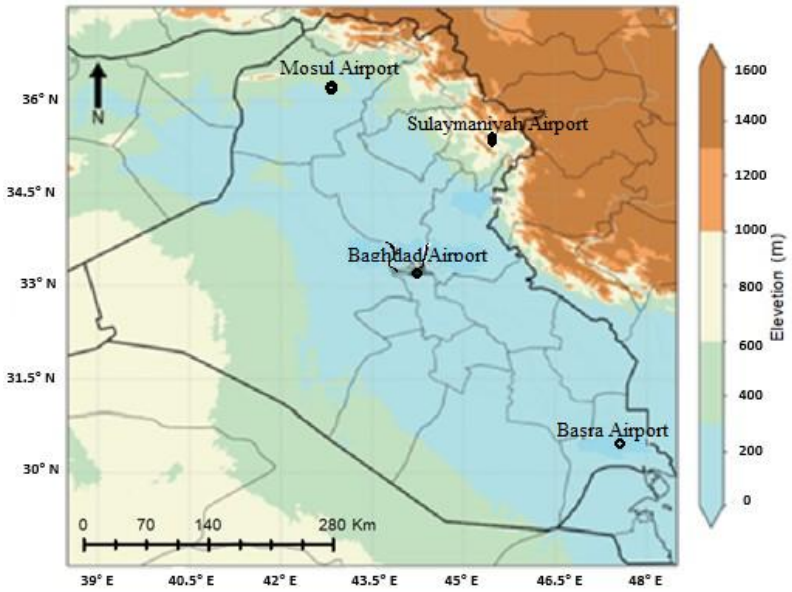



**Figure 1.** Map of Iraq with the selected stations (Al-Khulaifawi & Ioshpa, 2025)

## 2.2. Data Sources and Methodology

### 2.2.1. Meteorological Station Observations

Real-time surface monitoring data were obtained in real time from the Iraqi General Authority for Meteorology and Seismic Monitoring for an extended period of 16 years (2010–2025). Data extracted included hourly frequency of thunderstorms, surface air temperature (T), dew point temperature (Td), relative humidity (RH), surface atmospheric pressure (PPP), and wind speed (FF). These variables were collected at the four main concurrent hours of local time (00:00, 06:00, 12:00, and 18:00) to represent four main meteorological stations covering the geographical and climatic diversity of Iraq: Baghdad Airport, Basra Airport, Mosul Airport, and Sulaymaniyah Airport; the data were collected from the four weather stations, as shown in Table 1. Baghdad's climate is classified as a hot semi-desert climate. Summers are very hot and very dry, with maximum averages ranging between 43°C and 48°C, and may exceed 50°C in July and August. Winters are relatively cold to moderate, and rainfall is low and variable, with an annual rate ranging from 120 to 150 mm (Al-Khulaifawi and Mutar, 2026). Basra's climate is categorized as an arid-desert climate, with scorching summers that can reach temperatures of above 50°C and mild to chilly winters with little precipitation. The city's close proximity to the Arabian Gulf contributes to its excessive humidity (Al-khulaifawi & Ioshpa, 2025; Shukur, 2025). Mosul exhibits a hot semi-arid climate, adjacent to a Mediterranean climate, characterized by intensely hot, arid summers and moderately wet, comparatively chilly winters (Chen & Chen, 2013). The mean summer temperature ranges from 30 to 46 degrees Celsius, while the average precipitation is approximately 354 millimeters (Ali, 2020). The Sulaymaniyah region exhibits a continental arid (Mediterranean) climate characterized by hot, dry summers; chilly winters; and elevated evaporation rates in summer attributed to high temperatures and very low humidity, while the annual precipitation rate reaches about 796 mm (Ali et al., 2015). Surface data was subjected to both manual and automatic quality assessments to eliminate any anomalous or irrational values. Absence of data in surface observations was addressed with the utilization of reanalysis data.

**Table 1:** Weather Station Information.

| Station | Station number | Longitude | Latitude | Height (m) |
|---|---|---|---|---|
| Baghdad Airport | 650 | 44.24° N | 33.18° E | 31.7 |
| Basra Airport | 690 | 47.47° N | 30.31° E | 2.6 |
| Mosul Airport | 608 | 43.15° N | 36.32° E | 223 |

| | | | | |
|---|---|---|---|---|
| Sulaymaniyah Airport | 623 | 45.45° N | 35.53° E | 843 |

### 2.2.2. Reanalysis Data

Data were extracted from NCEP/NCAR and MERRA-2 for values of particulate matter (PM2.5), total precipitable water (TPW), cloud top temperature (CCT), and Integrated water vapor transport (IVT) as well as extracting CAPE values calculated vertically from the surface up to the equilibrium level for each station. The used model (NCEP/NCAR) from the Physical Sciences Laboratory global reanalysis dataset has a spatial resolution of 0.25° × 0.25° for the atmosphere, and variables were extracted matching exactly the closest of the four daily synoptic analysis hours (03:00, 09:00, 15:00, or 21:00 UTC) with a temporal resolution for the interval 2010–2025 (Kalnay et al., 1996). The model synopsis is summarized in Table 2.

The Modern-Era Retrospective analysis for Research and Applications, version 2 (MERRA-2), is a comprehensive atmospheric reanalysis dataset produced by NASA's Global Modeling and Assimilation Office (GMAO). Introduced in 2017, MERRA-2 provides extensive atmospheric data, including a continuous aerosol record from 1980 to the present. The dataset offers a spatial resolution of 0.5° by 0.625° and incorporates 72 vertical layers extending above 80 km. These features result from integrating the Goddard Earth Observing System, version 5 (GEOS-5) model with the Goddard Chemistry, Aerosol, Radiation, and Transport (GOCART) model (Buchard et al., 2017; Colarco et al., 2010).

Due to the difference in time frames between local ground station records and NCEP modeling hours subtracted every 6 hours (03:00, 09:00, 15:00, and 21:00 UTC), a strict time match was constructed; UTC was converted to local time for ground stations, and temporal matching was performed to the nearest synchronized observation hour (synoptic hour), ensuring that the time gap was reduced to a minimum to ensure physical comparison during the emergence and development of thunderstorms hour by hour.

In order to reduce spatial uncertainty and address variation in network resolution between microgrid MERRA-2 model products (0.5° × 0.625°) and more extensive NCEP/NCAR model fields (2.5° × 2.5°), a rigorous protocol (spatial downscaling) was applied. All air transactions (CAPE, IVT, CCT, and TPW) were spatially standardized over the exact geographic coordinates of the four ground airport stations using the bilinear spatial interpolation technique. This interpolation method calculates the weighted average of weather variables from the four network nodes closest to and surrounding the location of each station (Baghdad, Basra, Mosul, and Sulaymaniyah). By implementing this spatial smoothing, subgrid gradients were systematically constrained, preventing artificial spatial discontinuities at grid cell boundaries and ensuring a sound physical match between topography-stimulated ground observations and vertically integrated reanalysis models.

**Table 2:** Overview of the ERA-5 driving model.

| Characteristics | MERRA-2 | NCEP/NCAR |
|---|---|---|
| Horizontal coverage | Global and local | Global |
| Vertical coverage | 1000 to 0.1 hPa | 1000 hPa to 10 hPa |
| Outputs | each 3h for upper air | each 6h for upper-air |
| Horizontal resolution | 0.5° × 0.625° | 2.5° × 2.5° |
| Vertical resolution | 42 pressure levels | 17 pressure levels |
| Data assimilation | Yes | Yes |

This investigation uses bias-corrected global hourly surface PM2.5 mass concentration data from 2010 to 2025. This data was created for the NASA Health and Air Quality Applied Sciences Team (HAQAST) using a convolutional neural network (CNN)-based machine learning technique (Gupta & Sayeed, 2024). The following Table 3 provides specifics on the classification criteria for PM2.5 concentrations:

**Table 3:** Classification of PM2.5 concentrations (Al-khulaifawi & Ioshpa, 2025; EPA, 2018).

| PM2.5 | concentration (µg/m³) |
|---|---|
| A | (0-12) |
| B | (12.1-35.4) |
| C | (35.5-55.4) |
| D | (55.5-150.4) |
| E | (15.5-250.4) |
| F | (250.5-500.4) |

### 2.2.3 Data Processing, Filtering, and Statistical

The combined data underwent a series of standard procedural steps before being subjected to statistical analysis to ensure the quality of physical inference:

- Load power value filtering (CAPE): All CAPE values less than 300 J/Kg are excluded and deleted. Physically, this exclusion is due to the fact that the lower energies do not have sufficient dynamic capacity to stimulate the upward air currents (updrafts) needed to generate convective thunder cells, and rooting this condition isolates stable states that disrupt real storm modeling.
- Filtering of integrated water vapor transport (IVT) values: Cases where the integrated water vapor transport values were zero (IVT = 0) were excluded because the absence of horizontal or vertical flow of water vapor moisture completely cuts off the wet feed from the atmospheric column, preventing the formation of cumulonimbus clouds.
- Statistical analysis and multiple regression model: The nature and strength of the linear cross-effect relationships between TPW and PM2.5 and thermodynamic coefficients were evaluated using the Pearson linear correlation coefficient. Based on the independent correlation outputs, the relationships were combined into a multiple linear regression model to construct an innovative estimated mathematical equation for the precipitation water content (TPW Est) as follows:

$$TPW\ Est = a + \ \mathrm{b} * (\mathrm{PM2.5}) + \ \mathrm{b} * (\mathrm{CCT}) + \ \mathrm{b} * (\mathrm{CAPE}) \ + \ \mathrm{b} * (\mathrm{IVT})$$

Where (a) represents the fixed limit of the cutoff, and the coefficients (b) represent the regression weights and statistical slope of each variable balanced for each independent meteorological station. The comprehensive operational steps of data acquisition, temporal collocation, quality filtering, and statistical modeling are systematically illustrated in the methodological flowchart (Figure 2).

With the aim of evaluating the diagnostic efficiency and verifying the mathematical reliability of innovative multiple linear regression equations in estimating total water content ($TPW_{Est}$) compared to actual observed values ($TPW_{Obs}$), two standard statistical error measures were included: MAE (mean absolute error) as in the equation and RMSE (root mean squared error) as in the equation (Chai & Draxler, 2014). The MAE measures the average magnitude of absolute deviations between estimated and real values to provide a direct linear assessment of model accuracy, while the RMSE is used for its high sensitivity to large or anomalous errors (outliers) by squaring the differences, allowing the detection of the stability and efficiency of proposed mathematical equations during severe weather disturbances and extreme thunderstorms. These indicators were collected and calculated for each of the four stations and included in Table 5.

$$MAE = \frac{1}{\mathrm{N}} * \sum_{i=1}^{n} \left| TPW_{Obs,i} - TPW_{Est,i} \right|$$

$$RMSE = \sqrt{\frac{1}{N} * \sum_{i=1}^{n} \left(TPW_{Obs,i} - TPW_{Est,i}\right)^2}$$

- Where (N) represents the total size of the sample of thunderstorm days observed at the station.

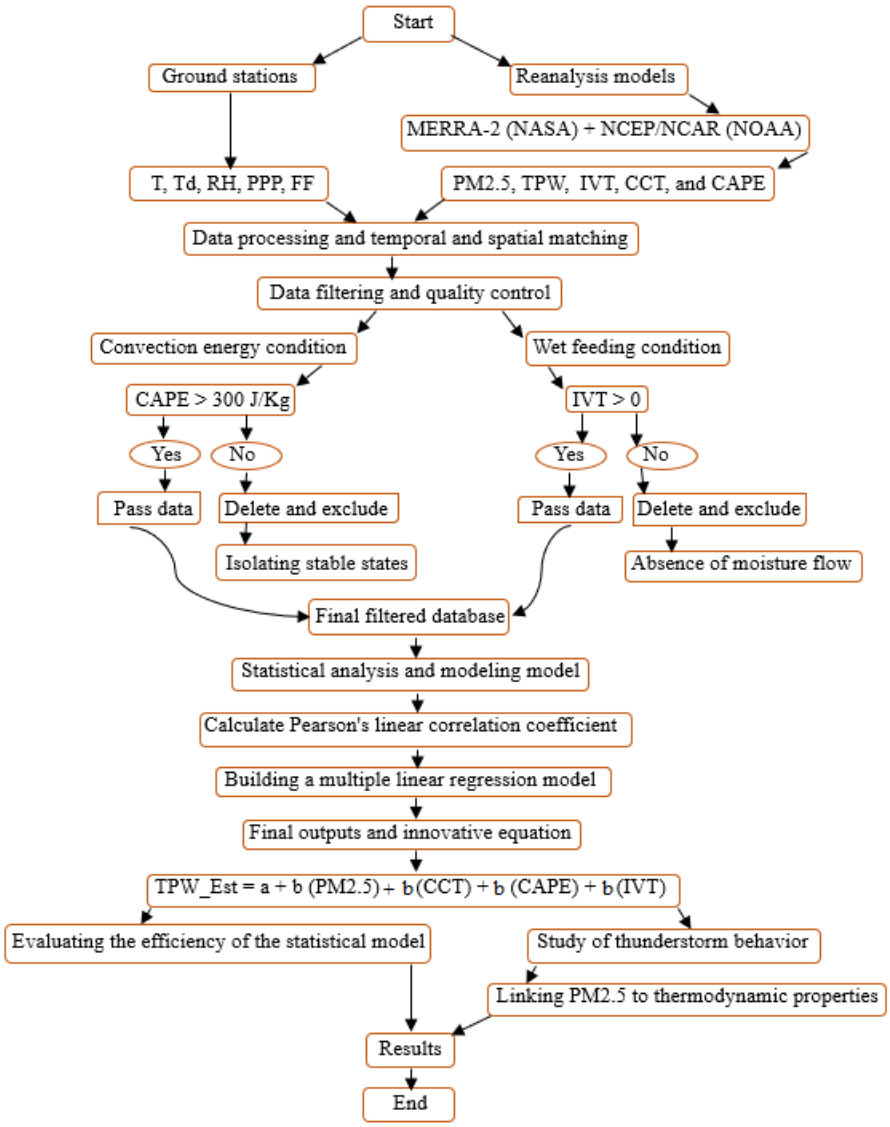



**Figure 2.** The methodological flowchart for 4 stations (2010-2025)

## 3. Results and Discussion

### 3.1. Analysis of the Nature and Distribution of Thunderstorms With the Main Observation Time

Figure 3 shows the temporal distribution of the annual frequency of thunderstorms over Baghdad, Basra, Mosul, and Sulaymaniyah Airport Stations for the period (2010-2025) and for the following times (00:00, 06:00,

12:00, and 18:00), where thunderstorms were recorded for 137 days (160 cases), 92 days (98 cases), 117 days (119 cases), and 261 days (301 cases), respectively. The figure indicates that the number of thunderstorms fluctuated significantly from year to year; this fluctuation reflects the changing nature of the meteorological factors influencing the formation of thunderstorms, which are directly related to the dynamic and thermal conditions of the atmosphere in the region. The total number of annual thunderstorm days varied widely during the study period, with a minimum value of 2 days (in 2021), 2 days (in 2012 and 2021), 1 day (in 2021), and 6 days (in 2015), respectively. The maximum values are 20 days (in 2018), 13 days (in 2018), 17 days (in 2011), and 28 days (in 2014), respectively. The total average number of days of annual thunderstorms varies from one station to another, depending on the nature of the topography (plain area or mountain) of each station and its frequent exposure to grooves and depressions that cause the phenomenon of thunderstorms to recur, with large fluctuations around this average.

This variability is a critical factor to consider when assessing extreme weather risks and infrastructure planning and requires deeper statistical analysis to link these cycles to larger-scale climate factors (such as climate oscillations or the El Niño/La Niña phenomenon). However, continued monitoring and analysis of thunderstorm data over longer timescales and linking them to factors such as surface humidity, lower atmosphere temperatures, and atmospheric pressure distribution may help clarify future trends in thunderstorm activity in the region. In 2005 and 2008, the least frequent thunderstorms were witnessed, while in contrast, these two years witnessed the highest frequency of dust storms in Baghdad (Mohammed & Hassoon, 2019). The results showed a negative relationship between dust storms and the El Niño phenomenon. This means that Iraq experiences more dust storms during La Niña periods and fewer during El Niño periods (Al-Qadi et al., 2021). Rain and thunderstorms remove particles from the air, which, in some circumstances, might result in a drop in PM2.5 that persists after the storm. The area, the time of year, and the pollution sources all affect this (Al-Khulaifawi & Ioshpa, 2026). Thermodynamic instability is strongly connected with stroke counts in thunderstorms, and aerosol effects on thunderstorms are strong and can enhance lightning when considered in conjunction with instability (Sae-Jung et al., 2025).

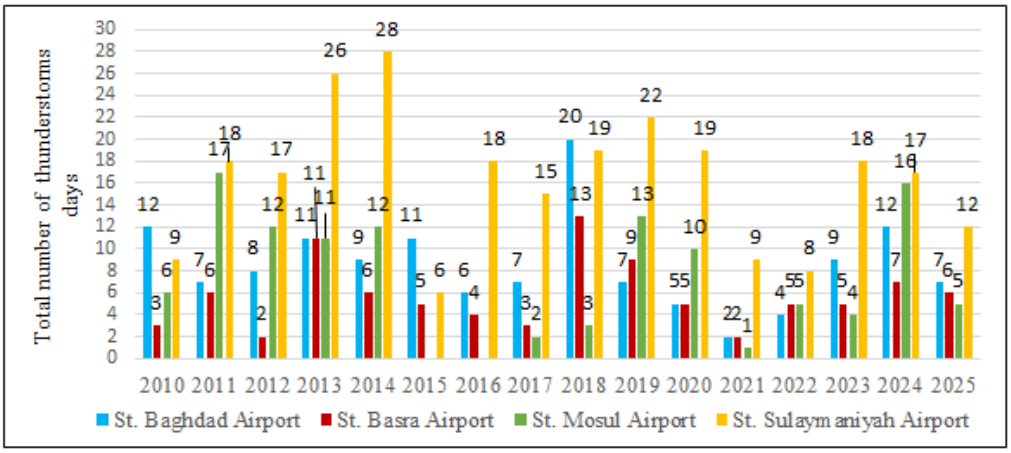



**Figure 3.** Annual distribution of thunderstorms for the period 2010-2025

On the other hand, thunderstorms are more frequent throughout the country in spring (April) (Al-Khulaifawi & Ruvimovich, 2025; Al-Khulaifawi & Ioshpa, 2025). Figure 4 illustrates the monthly distribution of thunderstorm frequency at four stations from 2010 to 2025 (January, February, March, April, May, September, October, November, and December). Analysis reveals a pronounced seasonal variation, with the majority of thunderstorms occurring in the spring and fall. Peak activity is observed in April at Baghdad, Mosul, and Sulaymaniyah Airport Stations, while at Basra Airport Station, it was recorded in April and November; the number of cases reached 29, 41, 57, and 21 storms, respectively (Al-Khulaifawi & Ioshpa, 2026; Al-Khulaifawi & Mutar, 2026). Reflecting a rise in atmospheric instability rates in the spring and fall due to the collision of warm, humid air masses from lower latitudes with cold air masses from higher latitudes, no thunderstorms were recorded or observed during the summer at four stations.

At Baghdad Airport Station during the spring period (main peak), the highest levels of thunderstorm frequency occur in the spring (54%), recording the highest total value ever in April. This is followed by March (23 days). In the fall season (second peak), it reached 33.60%. These conditions are typically attributed to the strong interaction between advancing warm, humid air masses and unstable atmospheric systems between high and low latitudes. These conditions lead to enhanced convection and the formation of cumulonimbus clouds, which are responsible for thunderstorms.

At Basra Airport Station during the spring season, thunderstorms occur most frequently, with a peak frequency of 56.52% recorded in April, marking the highest overall value ever. This is followed by May (17 days). In the fall season (second peak), it reached 29.35%.

At Mosul Airport Station during the spring period (main peak), the highest frequency of thunderstorms occurs in the spring (67.52%), recording the highest overall value ever in April. The second peak, which reached 16.24%, was shared between the fall and winter.

At Sulaymaniyah Airport Station during the spring period (main peak), the highest frequency of thunderstorms occurs in the spring (54.41%), recording the highest overall value ever in April. This is followed by May (43 days). In the winter season (second peak), it reached 23.37%.

In contrast, September was the least active month for Sulaymaniyah Airport, with nearly six storms recorded. This is due to the dominance of subtropical highlands in the summer months, which stabilizes the atmosphere and prevents the development of cumulus clouds (i.e., fewer thunderstorms). While January was the least active month for Baghdad Airport (5 storms) and Basra Airport (2 storms) and for Mosul Airport, December was the least active month, recording nearly 3 storms, reflecting some instability associated with the cold fronts of mid-latitude depressions.

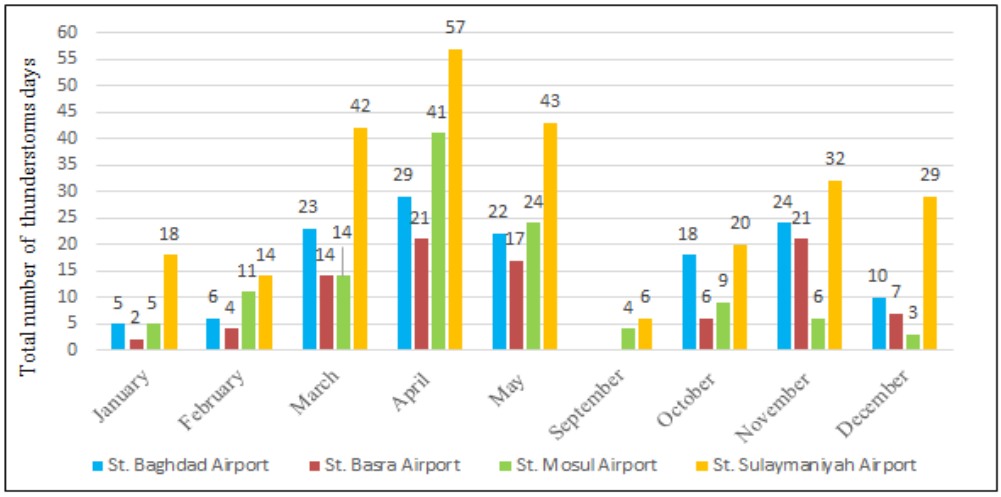



**Figure 4.** Monthly distribution of thunderstorms for the period 2010-2025

By analyzing nine months of data for the Baghdad, Basra, Mosul, and Sulaymaniyah Airport Stations, the results showed that the best time for thunderstorms to recur is 18:00. The lowest time for thunderstorms at Baghdad Airport Station is 06:00, and at Mosul and Sulaymaniyah Airport Stations, it is 12:00, while at Basra Airport Station, it is 06:00 and 12:00.

## 3.2. The Impact of Thunderstorms on PM2.5 in Iraq

Results of the impact of thunderstorms on PM2.5 and their frequencies are presented in Figures 5-8 and summarized in Table 4. These results are based on PM2.5 concentrations before, during, and after the thunderstorms

at Baghdad, Basra, Mosul, and Sulaymaniyah Airport Stations and by using hourly data of thunderstorms (wet and dry) for 9 months (January, February, March, April, May, September, October, November, and December) for the period from 2010 to 2025.

Figure 5 shows that the concentration of PM2.5 at Baghdad Airport Station is at two levels: the (C) and (D) groups in varying proportions. The reason is the lack of high humidity in the air (lack of rain). Another reason is that this is the result of the wind bringing dust from western Iraq (the desert), and there are millions of cars and many power generators in Baghdad, in addition to urban development and the bulldozing of agricultural land due to drought and lack of rain. Therefore, not all thunderstorms are accompanied by rain (the reason is that there is not enough moisture in the atmosphere), so the concentration does not decrease to levels (A) and (B) due to the increase in the concentration of dust and pollutants as a result of the downdraft and updraft of thunderstorms with light or no rain. The concentration of dust (particulate matter 2.5) in the atmosphere has grown as a result of low relative humidity and the passage of a cold front (of high density), which stirs up the dust and holds it suspended for a while. At the observational level, there is a positive correlation between the frequency or intensity of thunderstorms and atmospheric PM2.5 concentrations above the surface. This is because thunderstorms mix up aerosols during the storm, create aerosol particles at high altitudes, and redistribute contaminants. Thunderstorms are also associated with local sources of smoke and dust, such as fires or construction dust, which may be exacerbated by the storm's atmospheric conditions (Al-khulaifawi & Ioshpa, 2026). Before, during, and after a thunderstorm: The majority of PM2.5 frequencies fall within the category of (D) prevailing frequency, recorded at approximately 56%. It is followed by ranges (C) and (E) with a slight decrease after a thunderstorm, while category (B) is the opposite (slight increase). Categories (D), (E), and (F) are considered unhealthy. It was noted at this station that category (F) increases even after a thunderstorm, which indicates the danger of air pollution in the atmosphere and that the rain was not sufficient to wash away or remove suspended particles from the atmosphere.

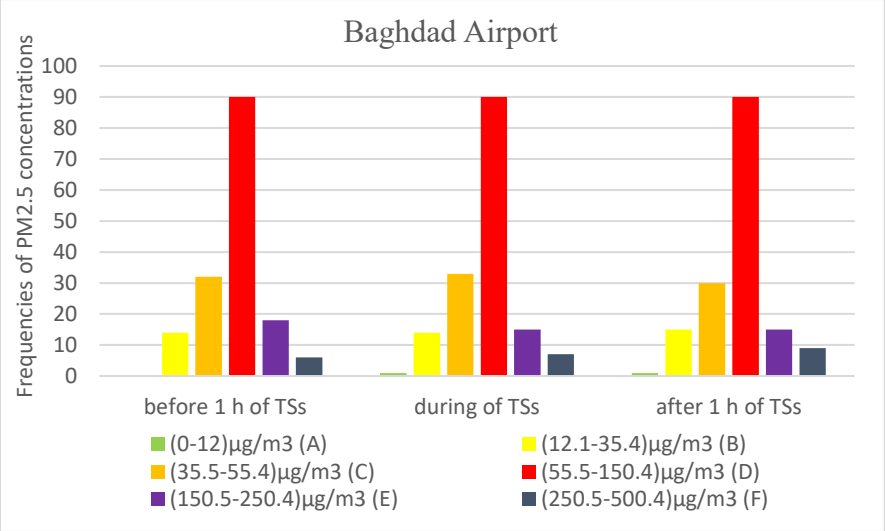



**Figure 5.** Temporal analysis of air quality status mean frequencies of PM2.5 concentration levels (nine months, 2010-2025) for Baghdad Airport Station

Figure 6 shows that the concentration of PM2.5 at Basra Airport Station is at three levels: the (D), (E), and (F) groups in varying proportions. Recently, high concentrations of air pollution have been recorded as a result of petrochemical plants, and this city is characterized by a large number of oil wells, power plants, brick and asphalt factories, steel and iron foundries, waste incineration, agricultural land removal, burning of crude oil and gas, and vehicle exhausts. Before, during, and after a thunderstorm: The majority of PM2.5 frequencies fall within the category of the prevailing frequency (D), recorded at approximately 51%. Ranges (E) and (F) show a slight decrease after a thunderstorm, while category (C) exhibits a slight increase. It was noted at this station that categories (E) and (F)

represent 35%, which indicates the seriousness of air pollution in the city's atmosphere; due to the lack of rain and the increased frequency of dust storms, this station is considered more dangerous in terms of air pollution. The elevated concentrations of PM2.5 in Baghdad and Basra pose a health hazard. The article advocated for the implementation of stringent environmental measures to mitigate air pollution, including enhancing manufacturing efficiency and promoting the utilization of clean energy. It underscored the necessity establishing air quality monitoring systems and enacting measures to mitigate harmful emissions in urban and industrial regions (Atheeb, 2025). The results indicated that PM2.5 concentrations were higher in summer than in winter and autumn. The average monthly maximum concentration was 8.4 μg/m³ in June and 8.7 μg/m³ in July, particularly in the central and southern regions of Iraq. The seasonal average concentration followed a similar pattern to the monthly pattern, with its highest values reaching an average of 7.1 μg/m³ in summer. The annual average PM2.5 concentrations in Iraq are lower than the internationally recommended maximum of 10 μg/m³, reaching 6 μg/m³ (Sardar et al., 2023).

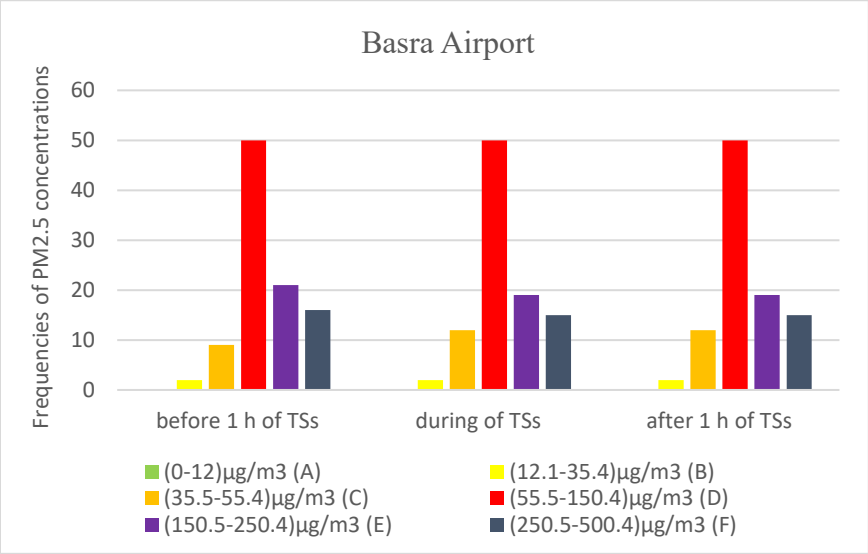



**Figure 6.** Temporal analysis of air quality status mean frequencies of PM2.5 concentration levels (nine months, 2010-2025) for Basra Airport Station

The results shown in Figure 7 indicate that the (B) level accounts for the frequency of PM2.5 at Mosul Airport Station. This is because of large areas of agricultural land and not many asphalt plants and oil wells in the city. Additionally, a smaller population and fewer cars and generators. Therefore, the concentration of PM2.5 is low (indicating clean or moderate air). Before, during, and after a thunderstorm: The majority of PM2.5 frequencies fall within the category of (B) prevailing frequency, recorded at approximately 43%. It is followed by range (D) with a slight decrease after a thunderstorm, while categories (A) and (C) are the opposite (a slight increase). It was noted at this station that categories (E) and (F) are represented in small proportions, which indicates the purity of the air in the city's atmosphere. It is considered the best station in terms of air pollution, as the concentrations of suspended particles accompanying thunderstorms were recorded as acceptable.

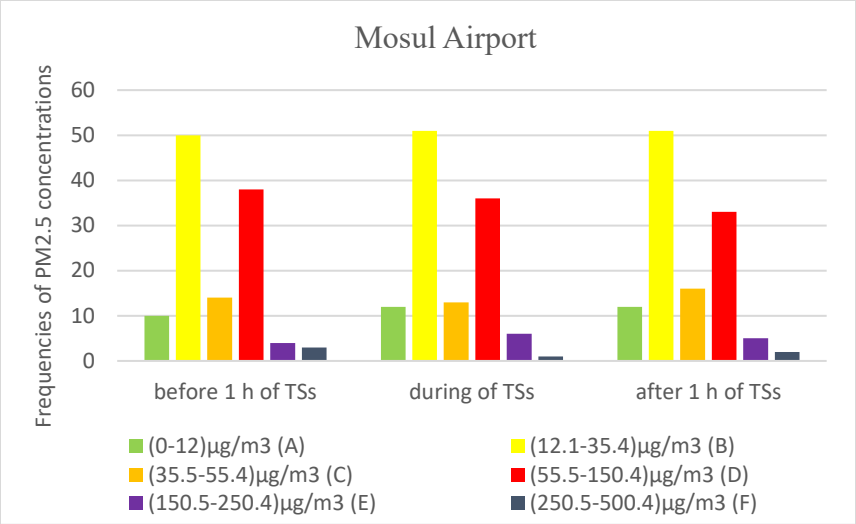



**Figure 7.** Temporal analysis of air quality status mean frequencies of PM2.5 concentration levels (nine months, 2010-2025) for Mosul Airport Station

Figure 8 shows that the concentration of PM2.5 at Sulaymaniyah Airport Station is at three levels: the (B), (C), and (D) groups in highly varying proportions. This station is distinguished by its height above ground level exceeding 800 meters due to the mountainous terrain of the city. It is considered one of the areas with the most rain and snow from the southern regions, but despite that, unhealthy concentrations were recorded within category (D). Before a thunderstorm: The majority of PM2.5 frequencies fall within the category of (D) prevailing frequency, recorded at approximately 36.5%. During and after a thunderstorm, the majority of PM2.5 frequencies fall within the category of (B) prevailing frequency, recorded at approximately 39.4%. It is followed by category (C) (27%) with an increase after a thunderstorm, while category (A) (5%) has a slight increase. It was noted in this station that category (F) is represented by a small percentage. This does not indicate the purity of the air in the city's atmosphere because the concentration of category (A) is also low, along with a high concentration of category (D). Categories (E and F) were not observed during and after the thunderstorm, but only 20 cases were recorded before the thunderstorm. It is considered the second-best station in terms of air pollution after the Mosul station. Not all thunderstorms at the station are accompanied by rain (the reason is that there is not enough moisture in the atmosphere), so the concentration does not decrease to a level (A) due to the increase in dust and pollutants caused by the downdrafts and updrafts of thunderstorms.

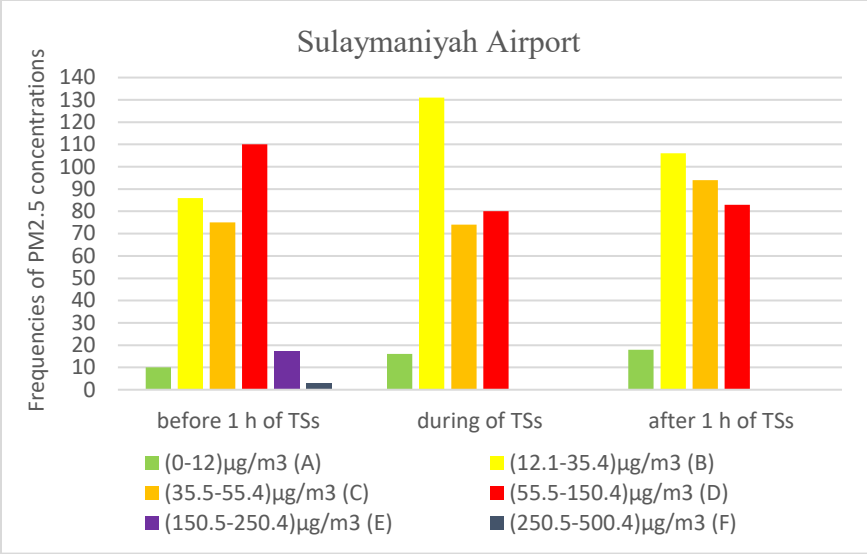



**Figure 8.** Temporal analysis of air quality status mean frequencies of PM2.5 concentration levels (nine months, 2010-2025) for Sulaymaniyah Airport Station

The statistical data in table 4 show significant geographic and climatic variation in the frequency and quality of thunderstorms and the behavior of particulate matter (PM2.5) concentrations across the four Iraqi airport stations studied (Baghdad, Basra, Mosul, and Sulaymaniyah). Sulaymaniyah Airport Station recorded the highest total frequency of thunderstorms at 261 cases, while Basra Airport Station recorded the lowest frequency at 92 cases. This spatial distribution is directly attributed to the topographical and climatic characteristics of Iraq; the mountainous highlands in the northern region (Sulaymaniyah) contribute to the stimulation of the dynamic uplift forces (orographic lifting) necessary for the development of the Mazniya cumulus clouds, compared to the plain and lowland regions in the center and south.

In terms of the association of storms with rainfall, the results indicate a clear superiority of cases accompanied by rain in Sulaymaniyah (161 cases), Baghdad (87 cases), and Mosul (76 cases), which reflects the efficiency of cloud systems in these regions in reaching maturity and liquefying vertical water content. In contrast, the storm rates were similar (45 rainy versus 47 non-rainy) at the Basra Airport Station, a behavior that is physically explained by the southern region being affected by the phenomenon of evaporation induced in the lower layers of the atmosphere under the cloud as a result of the high surface temperature, which leads to the evaporation of precipitation before it reaches the earth, or by the excitation of severe dust storms associated with dry fronts without the availability of sufficient moisture for condensation.

When these dynamics are linked to the behavior of air pollutants, patterns of fine particle concentrations (PM2.5) before, during, and after the storm (one hour apart) reveal two opposing physical mechanisms governed by the nature of the atmospheric system; the symbol (B) at the Mosul and Sulaymaniyah Stations represents the effect of wet deposition, as heavy rains and rising water molecules wash and cleanse the atmosphere of PM2.5 molecules, which leads to a sharp drop in their concentrations during and after the storm. In contrast, the symbol (D) in the stations of Baghdad, Basra, and Sulaymaniyah (before the storm) highlights the mechanism of mechanical dispersion and dust deflation resulting from the strong downward winds and wind shear forces accompanying thunderfronts, which lead to the resuspension of fine particles and the stirring of local dust, causing sharp jumps in concentrations of PM2.5, specifically in the semi-arid environment of central and southern Iraq, coinciding with the kinetic activity of the storms.

Table 4 indicates that the incidence of thunderstorms and wet days diminishes from north to south, whereas the greatest concentration of PM2.5 increases from south to north. This suggests that heightened rainfall results in reduced concentrations of PM2.5.

**Table 4:** Summarizes the results (thunderstorms and PM2.5) for four meteorological stations during the period (2010-2025).

| Stations | Total thunderstorm events | Events with rain | Events no rain | Maximum PM2.5 concentration before 1 h | Maximum PM2.5 concentration during 1 h | Maximum PM2.5 concentration after 1 h |
|---|---|---|---|---|---|---|
| **Baghdad Airport** | 137 cases | 87 cases | 50 cases | (D) | (D) | (D) |
| **Basra Airport** | 92 cases | 45 cases | 47 cases | (D) | (D) | (D) |
| **Mosul Airport** | 117 cases | 76 cases | 41 cases | (B) | (B) | (B) |
| **Sulaymaniyah Airport** | 261 cases | 161 cases | 100 cases | (D) | (B) | (B) |

- Most rainy cases recorded light rain at Baghdad, Basra, and Mosul Airport Stations.
- Most rainy cases recorded light and moderate rain at Sulaymaniyah Airport Station.

## 3.5. Analysis of the Relationship Between Total Precipitation Water and Parameters for 2010-2025

The Pearson correlation coefficient between the total precipitable water, PM2.5 concentration, cloud top temperature, CAPE, and integrated water vapor transport for 2010–2025 has been calculated for the study period. The results of Figure 9 show a clear direct linear (positive) correlation between the concentration of particulate matter (PM2.5) and the total precipitation water (TPW) in the atmosphere during frequent thunderstorms, which is statistically significant, as the correlation coefficients at Baghdad, Basra, Mosul, and Sulaymaniyah Airport Stations are R = 0.6, 0.63, 0.62, and 0.6, respectively. Despite the variation in maximum and minimum numerical ranges between these cities due to their topographic and climatic characteristics, the values of the total water content peaked at about 42 kg/m², coinciding with an increase in the concentration and mass density of particulate matter, which reached 60 kg/m² (Baghdad and Basra), while TPW values stopped at 33 kg/m² in Mosul and Sulaymaniyah. This is due to the mountainous and elevated topography of the northern region and the lower surface temperatures compared to the center and south, demonstrating the role of these pollutants as condensation nuclei that enhance water abundance within cloud systems. Fine particulate matter (PM2.5) acts as the "cloud condensation nuclei—CCN." As the masses of these particles in the air column increase, they attract and absorb surrounding moisture particles and water vapor from the surrounding atmospheric environment, which statistically and physically leads to an increase in the accumulation of vertically stored water mass and thus higher TPW values. In addition, this relationship is connected to the weather conditions that are associated with instabilities. High humidity contributes to an ideal environment for aqueous chemical reactions that stimulate the production and accumulation of secondary aerosols, demonstrating a reciprocal role in which suspended pollutants contribute to modifying the total water content available in the atmospheric system. Aerosols function as cloud condensation nuclei (CCN) or ice nucleating particles (INP), altering the physical and radiative characteristics of clouds and influencing precipitation formation processes (Albrecht, 1989; Liou & Ou, 1989; Twomey, 1977). Water vapor, an essential meteorological element in the troposphere, profoundly influences planetary energy and the hydrological cycle. Simultaneously, water vapor also affects the fluctuation of PM2.5 (Abdullaev et al., 2014; Zhang et al., 2017). Elevated humidity, sometimes associated with moist deposition from precipitation, diminishes PM2.5 levels, although augmented water vapor directly increases total precipitable water. Using inexpensive particulate matter sensors (Plantower PMS5003), mass concentrations of particulate matter (PM 1, PM 2.5, and PM 10) were measured at various elevations (1.5, 3, 9, 15, 18, and 290 m) in Tehran in order to

investigate their vertical distribution. Overall, the average PM2.5 values were 62.9 ± 44.7, 64.4 ± 46.6, and 66.6 ± 45.8 μg $m^{-3}$. As a result, changes in particulate matter concentrations with increasing altitude were statistically more significant during the day than at night, when air instability was present (Roostaei et al., 2024). Green plants may help purify the air and increase humidity in the atmosphere (although to a limited extent), and low population density in cities is one factor that leads to low concentrations. Latitude, longitude, sun altitude, solar radiation intensity, and topography all influence temperature. The higher the temperature, the higher the likelihood of PM2.5 concentrations and total precipitable water.

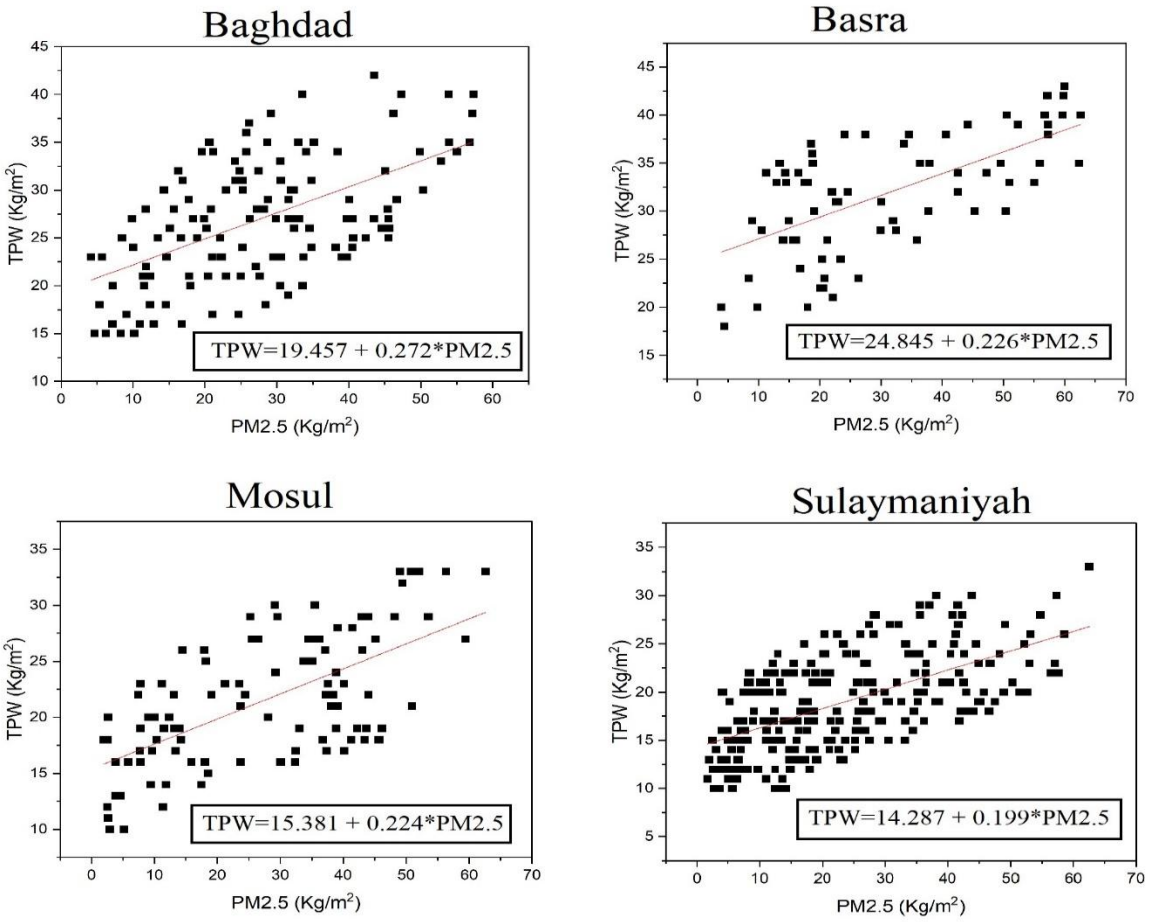



**Figure 9.** The correlation coefficient between particulate matter concentration PM2.5 and total precipitation water at all stations (2010-2025)

The results of Figure 10 show a moderate to strong inverse linear correlation for Baghdad, Basra, Mosul, and Sulaymaniyah Airport Stations (R = -0.56, -0.8, -0.77, and -0.52, respectively) between cloud top temperature (CCT) and total precipitation water (TPW); the decrease in cloud top temperatures (reflecting an increase in their vertical thickness and depth) was accompanied by a significant increase in the total water content to about 42 kg/m² at extremely cold temperatures (ranging between -60°C and -70°C), which was a direct indicator of the vertical growth and development of clouds and their reaching the upper layers of the atmosphere (the upper troposphere). This sharp vertical dynamic growth cannot occur without continuous wet feeding and massive pumping of water vapor through the entire air column, which explains the statistical synchronization between the temperatures of the cooler peaks and the highest values of the total water content available for precipitation, which approached 42 kg/m². In Basra specifically, proximity to water bodies (the Arabian Gulf) leads to an abundance of rising water vapor, enhancing the

vertical thickness of the drag and improving the dynamic cooling of the tops. While in Mosul and Sulaymaniyah stations, TPW values reach 33 kg/m², and this variation is due to the mountainous and high topography of the northern region's surface; cold and sea-level rise contribute to reducing the absolute carrying capacity of the air column for storing water vapor compared to the central and southern regions. These results are consistent with atmospheric physical explanations that confirm that the dynamic cooling associated with the decrease in CCT acts as an ideal environment to enhance the processes of condensation and water diffusion and stimulate the growth of water droplets and ice crystals due to the abundance of TPW. This increases the overall efficiency of the cloud system and demonstrates the role of dynamic cooling in stimulating the growth of water droplets through diffusion and collision mechanisms. The augmentation of cloud depth results in an elevation of total precipitable water due to the prolonged vertical motion of droplets inside the cloud parcel, hence enhancing the likelihood of growth through moisture diffusion and the processes of collision and coalescence. The TPW will be augmented (Mutar, 2024).

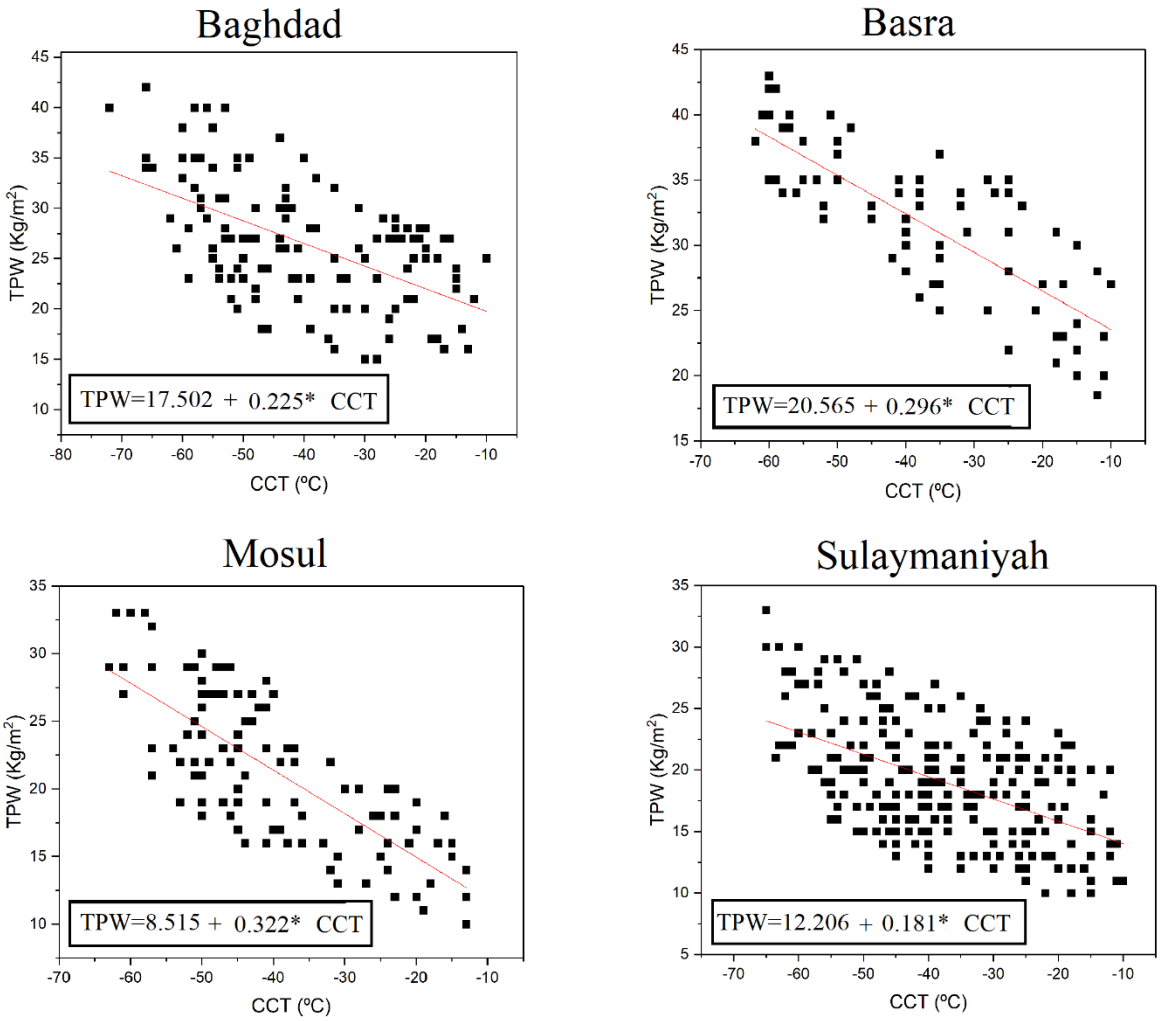



**Figure 10.** The correlation coefficient between cloud top temperature and total precipitation water at all stations (2010-2025)

The results showed a statistically significant direct linear correlation relationship between the convective available potential energy (CAPE) and the total precipitation water (TPW) as in Figure 11 (deleting values of CAPE less than 300), where the correlation coefficient values at Baghdad, Basra, Mosul, and Sulaymaniyah Airport Stations

reached R = 0.63, 0.7, 0.66, and 0.61, respectively. This positive proportionality is attributed to the role of atmospheric dynamic instability in stimulating updrafts that raise water vapor and increase the total stored vertical water content.

This dynamic and thermal correlation can be explained from the perspective of atmospheric physics by saying that the TPW represents the total vertical water stock in the air column and serves as the "real fuel" to feed the convection cells. When high TPW values are observed, the water vapor mixing ratio (w) in the lower atmosphere increases, which raises the default temperature of the ascending air parcels (Tv) compared to the surrounding dry environment. This thermal variation enhances the vertical buoyancy force and the growth of dynamic lift forces, thus causing the release and increase of stored CAPE potential energy, which peaked at more than 4000 J/kg, coinciding with the highest water content, reaching 42 kg/m². This physical mechanism is consistent with meteorological hypotheses that indicate that the intensification and instability of thunderstorms require an integrated system in which the TPW ensures abundant moisture, while the CAPE represents the engine and thermal catalyst to release this energy from moisture into heavy rain. A study by Gettleman et al. (2002) demonstrated a strong, linear positive correlation between vertical water content and thermal buoyancy energy in tropical and subtropical regions, where surface warming leads to increased evaporation (TPW) and energy feeding of convection cells (CAPE).

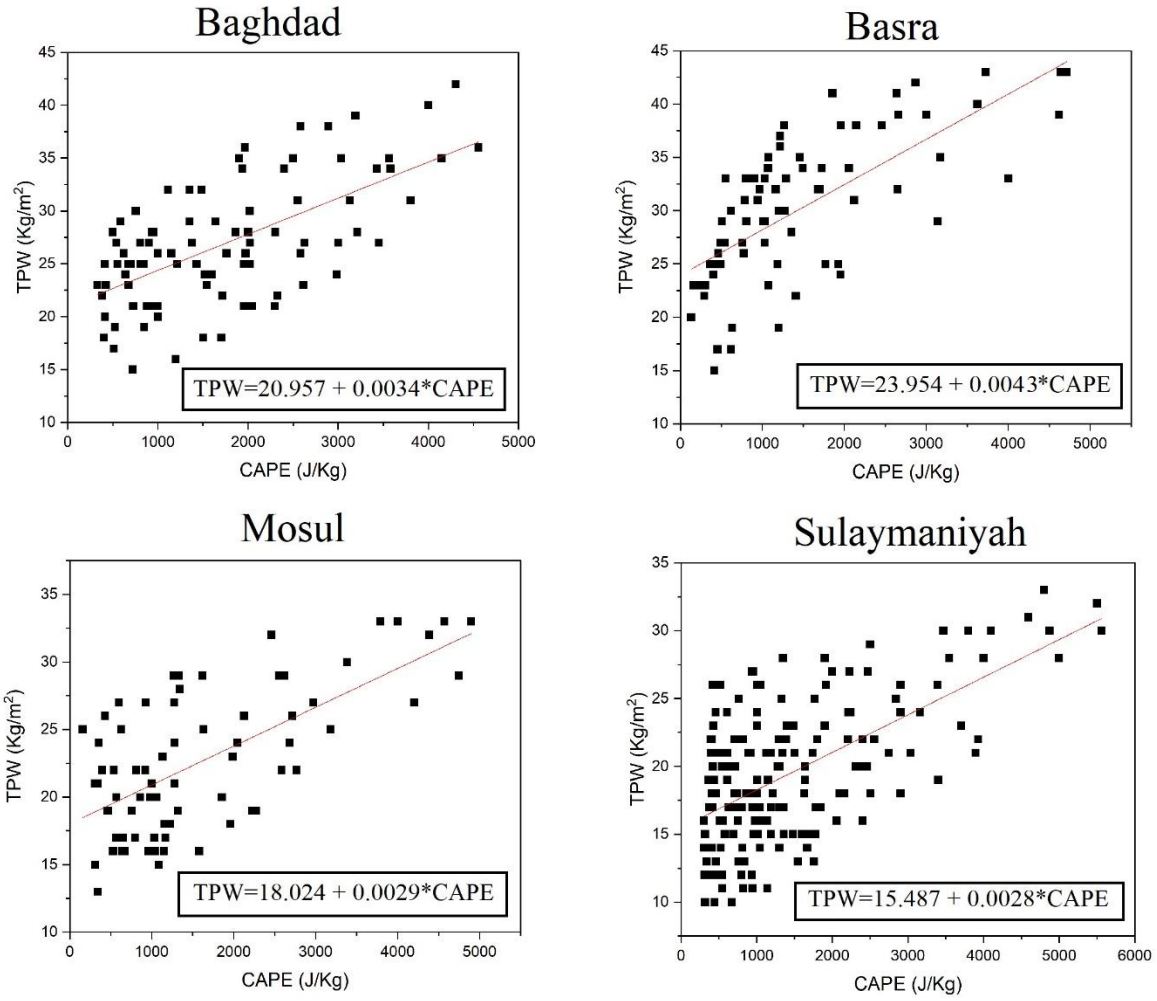



**Figure 11.** The correlation coefficient between convective available potential energy and total precipitation water at all stations (2010-2025)

The results of Figure 12 (deleting values where IVT = zero) revealed a direct linear correlation relationship between integrated water vapor transport (IVT) and total precipitation water (TPW), with the correlation coefficients for Baghdad, Basra, Mosul, and Sulaymaniyah airport stations (R = 0.6, 0.61, 0.77, and 0.7, respectively), demonstrating that intensifying the horizontal and vertical flow of water vapor directly contributes to raising the wet feed efficiency of the air column and increasing the total water content available for precipitation. This relationship can be explained in kinetic physical terms by the fact that IVT represents the horizontal and vertical flow of moisture carried by the wind through the lower layers of the atmosphere and serves as the nutritional dynamic mechanism that continuously pumps air masses saturated with moisture towards the study area. Accordingly, the intensification of this kinetic transport directly leads to the accumulation of water vapor molecules and an increase in their vertical mass density from the surface to the top of the troposphere, which is expressed physically by the growth of TPW values that peaked in the model at about 42 kg/m², coinciding with the recording of the highest rates of water transport at the stations of Baghdad Airport and Basra. This result is directly consistent with the dynamic concept published in the international literature of the formation of "atmospheric rivers," which proves that the static water abundance available for precipitation remains governed and constrained by the efficiency and strength of horizontal kinetic flows of incoming water vapor. Results indicate that 80 to 90% of the moisture captured by atmospheric rivers, along with a significant proportion of the overall precipitation generated by these systems, originates from tropical sources. The tropical contribution to precipitation generally exceeds 50% and significantly surpasses this figure in the most impacted regions (Eiras et al., 2017).

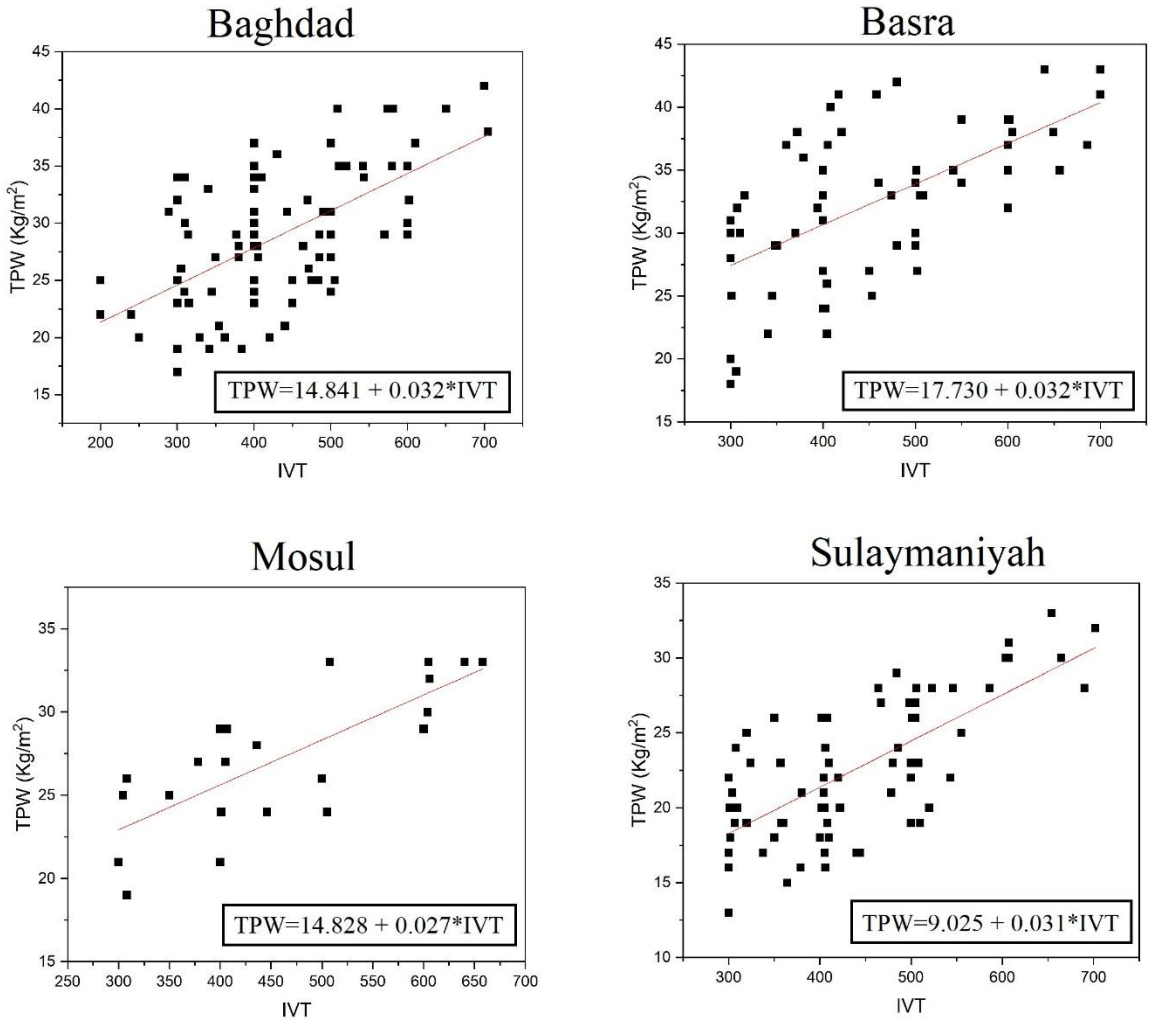


**Figure 12.** The correlation coefficient between integrated water vapor transport and total precipitation water at all stations (2010-2025)

To verify the accuracy and efficiency of numerical or computational models used to estimate atmospheric water content over the study area, this section represents an essential evaluation step for comparing experimentally inferred or estimated values with actual observed values. This step is of great importance in atmospheric physics, as the accuracy of determining the estimated total precipitable water (TPW $_{Est}$) is one of the cornerstones of ensuring reliable prediction of atmospheric instabilities. (TPW $_{Est}$) is calculated using the following equations:

$$TPW = a + b * PM2.5 \quad (1)$$

$$TPW = a + b * CCT \quad (2)$$

$$TPW = a + b * CAPE \quad (3)$$

$$TPW = a + b * IVT \quad (4)$$

By combining the above four equations, a multiple linear regression equation is produced to calculate (TPW $_{Est}$) based on the equations in the figures (9-12) for each station.

$$TPW\ Est = a + \ \mathrm{b} * (\mathrm{PM2.5}) + \ \mathrm{b} * (\mathrm{CCT}) + \ \mathrm{b} * (\mathrm{CAPE}) \ + \ \mathrm{b} * (\mathrm{IVT}) \quad (5)$$

$$TPW\ Est = 18.189 \ + \ 0.272 * (\mathrm{PM2.5}) + \ 0.225 * (\mathrm{CCT}) + \ 0.0034 * (\mathrm{CAPE}) \ +$$
$$0.032 * (\mathrm{IVT}) \quad \text{for Baghdad Station}$$

$$TPW\ Est = 21.774 + \ 0.226 * (\mathrm{PM2.5}) + \ 0.296 * (\mathrm{CCT}) + \ 0.0043 * (\mathrm{CAPE}) \ +$$
$$0.032 * (\mathrm{IVT}) \quad \text{for Basra Station}$$

$$TPW\ Est = 14.187 \ + \ 0.224 * (\mathrm{PM2.5}) + \ 0.322 * (\mathrm{CCT}) + \ 0.0029 * (\mathrm{CAPE}) \ +$$
$$0.027 * (\mathrm{IVT}) \quad \text{for Mosul Station}$$

$$TPW\ Est = 12.751 \ + \ 0.199 * (\mathrm{PM2.5}) + \ 0.181 * (\mathrm{CCT}) + \ 0.0028 * (\mathrm{CAPE}) \ +$$
$$0.031 * (\mathrm{IVT}) \quad \text{for Sulaymaniyah Station}$$

In Figure 13, the results extracted from the linear regression model show the existence of a direct (positive) correlation relationship from medium to strong between the estimated total precipitation water (TPW $_{Est}$) by equation 5 for each station and the actual total precipitation water (TPW), where the value of the correlation coefficient for the stations Baghdad Airport, Basra, Mosul, and Sulaymaniyah reached R = 0.7, 0.7, 0.77, and 0.73, respectively. The straight trend line (in red) reflects a typical convergence, showing that the higher the estimated values (TPW $_{Est}$) from 20 to 90, the more the actual documentation values (TPW) increase, reaching their peak at about 42 and 43 kg/m² for Baghdad and Basra Airport Stations and at 33 kg/m² for Mosul and Sulaymaniyah Airport Stations. This statistically confirms that the estimated model has good reliability, making it a consistent reference indicator that accurately reflects the wet structure of the air column in the study areas.

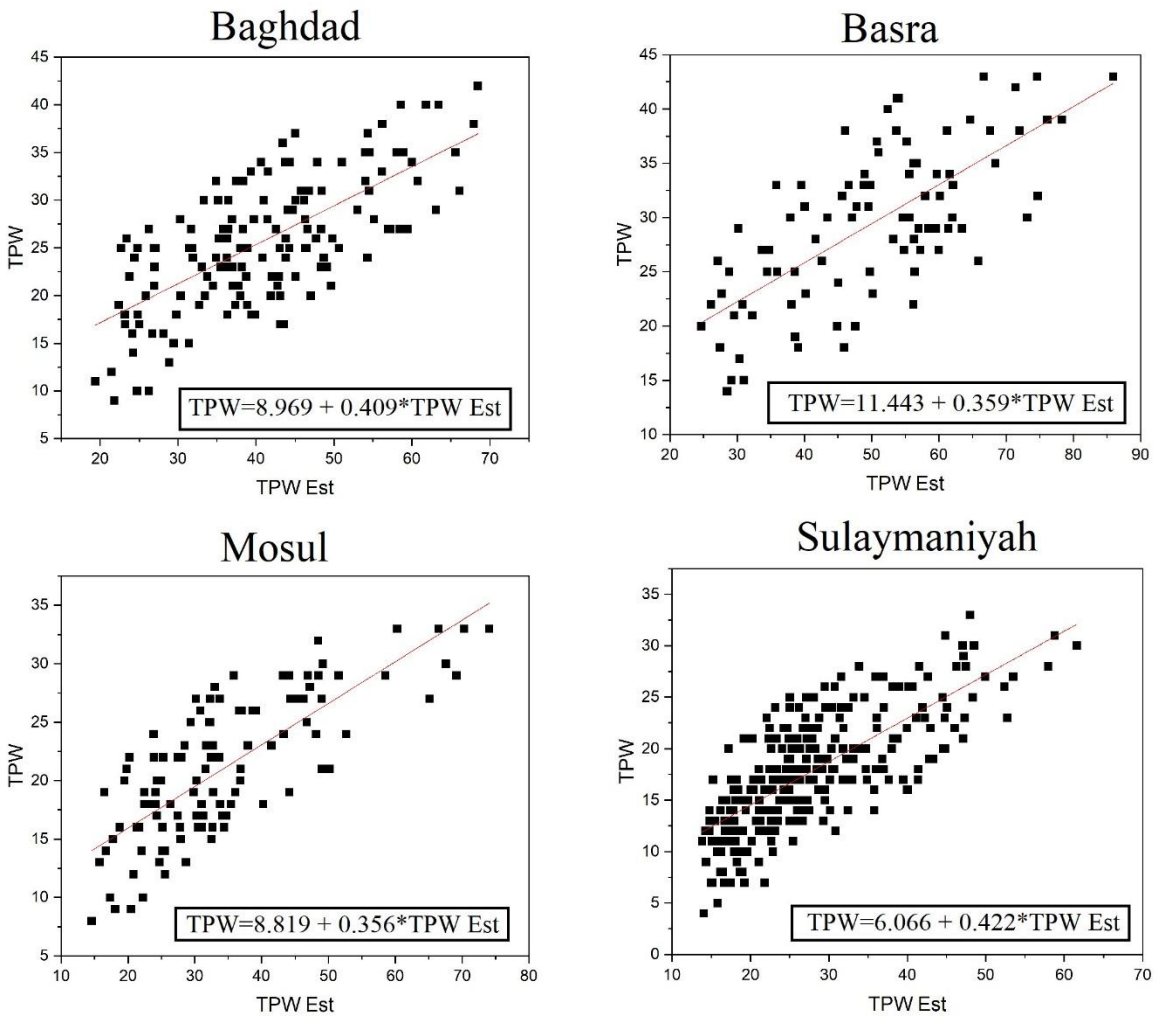



**Figure 13.** The correlation coefficient between estimated total precipitable water and total precipitation water at all stations (2010-2025)

Comparative statistical outputs between the four stations in Table 5 revealed clear physical and dynamic variation in the response of total precipitation water (TPW) to environmental and thermodynamic variables:

- (TPW and PM2.5): The highest direct correlation value was recorded at Basra Airport Station ($R = 0.63$, $R^2 = 0.4$), proving the high efficiency of atmospheric dust aerosols southward as moisture-attracting lenses and cloud condensation nuclei.
- (TPW and CCT): The highest sharp inverse correlation value was observed at Basra Airport Station ($R = -0.80$, $R^2 = 0.64$), followed by Mosul Station ($R = -0.77$), which physically explains why storms to the south and north are associated with towering vertical growth of cloud tops towards cooler layers of the atmosphere.
- (TPW and CAPE): The highest direct correlation value appeared at Basra Airport Station ($R = 0.70$, $R^2 = 0.5$) as a result of the high surface thermal heating that increases the buoyancy energy.
- (TPW and IVT): The relationship had the highest direct correlation value at the Mosul Airport Station ($R = 0.77$, $R^2 = 0.6$) due to its transition location affected by wet flows, while the lowest correlation value at the Baghdad Airport Station was recorded ($R = 0.60$, $R^2 = 0.4$).

Efficiency of the proposed mathematical model (TPWEst and TPW): The innovative multiple linear regression equation achieved the highest absolute diagnostic efficiency at the Mosul Airport Station ($R = 0.77$, $R^2 = 0.6$), confirming its successful physical integration of atmospheric determinants, while the lowest efficiency value (which remains a high and very scientifically acceptable value) was recorded at the Baghdad and Basra Airport Stations ($R = 0.70$, $R^2 = 0.5$).

The MAE and RMSE metrics showed higher predictive accuracy of the linear regression models at the northern stations (Sulaymaniyah and Mosul Airport Stations) compared to the southern stations, which is strong statistical evidence of the accuracy and stability of the model. Statistically, although these error magnitudes exceed 10 units, they are highly acceptable and representative of a strong simulation capacity given the wide dynamic range of the observed tropospheric TPW data. Crucially, the most compelling evidence of model stability is underscored by the remarkably tight and constant gap (~3 mm) maintained between MAE and RMSE across all distinct climatic zones. This convergence rigorously proves that the predictive residuals are normally distributed and free from severe anomalies or outlier errors. Physically, this is attributed to the effect of topographic uplift in the north versus the complexities of dry convection and dust in the south. The close proportionality between MAE and RMSE values across all stations indicates high structural stability of the model, proving its resistance to extreme values despite the intensity of weather fluctuations in the region.

**Table 5:** Results of the regression analysis of the linear relationship between the selected variables at four stations.

| Stations | Variables (Relationship) | a | b | R | $R^2$ | MAE | RMSE |
|---|---|---|---|---|---|---|---|
| Baghdad Airport | TPW and PM2.5 | 19.457 | 0.272 | 0.6 | 0.3 | | |
| | TPW and CCT | 17.502 | 0.225 | -0.56 | 0.3 | | |
| | TPW and CAPE | 20.957 | 0.0034 | 0.63 | 0.4 | | |
| | TPW and IVT | 14.841 | 0.032 | 0.6 | 0.4 | | |
| | $TPW_{Est}$ and TPW | 8.969 | 0.409 | 0.7 | 0.5 | 16.90 | 19.90 |
| Basra Airport | TPW and PM2.5 | 24.845 | 0.226 | 0.63 | 0.4 | | |
| | TPW and CCT | 20.565 | 0.296 | -0.8 | 0.64 | | |
| | TPW and CAPE | 23.954 | 0.0043 | 0.7 | 0.5 | | |
| | TPW and IVT | 17.730 | 0.032 | 0.61 | 0.4 | | |
| | $TPW_{Est}$ and TPW | 11.443 | 0.359 | 0.7 | 0.5 | 21.60 | 24.60 |
| Mosul Airport | TPW and PM2.5 | 15.381 | 0.224 | 0.62 | 0.4 | | |
| | TPW and CCT | 8.515 | 0.322 | -0.77 | 0.6 | | |
| | TPW and CAPE | 18.024 | 0.0029 | 0.66 | 0.4 | | |
| | TPW and IVT | 14.828 | 0.027 | 0.77 | 0.6 | | |
| | $TPW_{Est}$ and TPW | 8.819 | 0.356 | 0.77 | 0.6 | 13.48 | 16.15 |
| Sulaymaniyah Airport | TPW and PM2.5 | 14.287 | 0.199 | 0.6 | 04 | | |
| | TPW and CCT | 12.206 | 0.181 | -0.52 | 0.3 | | |
| | TPW and CAPE | 15.487 | 0.0028 | 0.61 | 0.4 | | |
| | TPW and IVT | 9.025 | 0.031 | 0.7 | 0.5 | | |
| | $TPW_{Est}$ and TPW | 6.066 | 0.422 | 0.73 | 0.5 | 10.45 | 13.07 |

## 4. Conclusions

Based on the thermodynamic and physical data and indicators for the period (2010–2025) in the various climatic zones of Iraq, the following main scientific conclusions were reached:

1. Topographic and dynamic stimulation of thunderstorms: The frequency of thunderstorms in Iraq shows sharp spatial variation governed by topographic determinants; The northern mountain highlands (Sulaymaniyah Station)

act as a distinct mechanical lifting mechanism that stimulates the formation of cumulus clouds to record the highest frequency of storms (261 days), while the southern plains and lowlands (Basra Station) record the lowest frequency (92 days). Seasonally, a peak convective activity was found during April and a complete absence of thunderstorms during the summer months.

2. Dual mechanism of wet deposition versus dust resuspension: The physical relationship between thunderstorms and fine particulate matter (PM2.5) reveals two opposing atmospheric mechanisms: In the northern and northwestern regions (Mosul and Sulaymaniyah), simultaneous rainfall activates a highly efficient "wet deposition and rainwashing" mechanism, reducing post-storm pollutant concentrations to an acceptable and moderate category (B). In contrast, dry load fronts dominate the dry and semi-arid environments of central and southern Iraq (Baghdad and Basra); strong downward winds and wind shear forces cause intense mechanical resuspension of topsoil, keeping air trapped in an unhealthy and dangerous category (D) before, during, and after the storm.
3. Thermodynamic coupling: The existence of a direct linear correlation between (PM2.5) and (TPW) provides conclusive experimental evidence that particulate pollutants and local industrial carbon emissions act as physically active "cloud condensation nuclei" (CCNs), accelerating the attraction and detection of surrounding water vapor molecules and increasing the abundance of vertically stored water mass in the atmosphere. The sharp inverse correlation between (CCT) and (TPW) confirms that the intense dynamic cooling of cloud tops depends physically on the continuous pumping of vertical moisture flows, allowing clouds to expand vertically and dynamically penetrate into the upper troposphere.
4. Diagnostic efficiency of the aggregate multiple regression model: Combining hydrodynamic parameters (PM2.5, CAPE, IVT, CCT) into a standardized multiple linear regression model has proven outstanding statistical success; the estimated equations achieved high stability and reliability with advanced correlation coefficients (R) ranging between 0.70 and 0.77 for all stations. The MAE and RMSE metrics showed a high predictive accuracy of the linear regression models at the northern stations compared to the southern stations, which is strong statistical evidence of the accuracy and stability of the model.

## 5. Conflict of Interest Statement

The authors declare that they have no conflicts of interest to report.


## 6. Funding Statement

This research did not receive any specific grant from funding agencies in the public, commercial, or not-for-profit sectors.


## 7. Author Contributions

"All authors contributed to the study conception and design. [Imad Abdulridha Jasim Al-Khulaifawi] and [Aqeel Ghazi Mutar] performed the material preparation, data collection, and analysis. The first draft of the manuscript was written, and all authors commented on previous versions of the manuscript. All authors read and approved the final manuscript."

## 8. Data Availability

"The datasets generated and analyzed during the current study are available in the NASA (MERRA-2) [https://giovanni.gsfc.nasa.gov/giovanni/] and NOAA (NCEP/NCAR) [https://psl.noaa.gov/data/atmoswrit/profile/]."

## References


Abdullaev, S.F., Maslov, V.A., Nazarov, B.I., & Salikhov, T.K. (2014). Water-vapor content in the atmosphere of arid zone. *Izvestiya, Atmospheric and Oceanic Physics, 50(2)*, 205-214. DOI: 10.7868/S0002351514010027

Albrecht, B. A. (1989). Aerosols, cloud microphysics, and fractional cloudiness. *Science*, 245(4923), 1227–1230. Doi: 10.1126/science.245.4923.1227

Al-Ansari, N. (2021). Topography and climate of Iraq. *Journal of Earth Sciences and Geotechnical Engineering*, 11(2), 1–13. http://doi.org/10.47260/jesge/1121

Ali, J.J.M., Nori, I.M., Hama, S.J., & Rashed, S.O. (2015). Water harvesting through utilization of wild almond as rootstocks for production of peach, apricot and plum under dry land farming in Sulaymaniyah region. *Int J Innovative Sci Eng Technol*, 2(8), 705–724. http://ijiset.com/vol2/v2s8/IJISET_V2_I8_92.pdf.

Ali S.H. (2020). Estimation of the land surface temperature for some districts in Nineveh Governorate by Landsat thermal imagery and GIS software. *Journal of Green Engineering*, 10(6), 3141-3155.

AL-Khulaifawi, Imad & Ioshpa, Alexander. (2025). Synoptic conditions and analysis of thunderstorm activity in Iraq and the Rostov region of Russia. *Geographical bulletin*. 126-133. 10.17072/2079-7877-2025-1-126-133

Al-khulaifawi, I. A., & Ruvimovich, I. A. . (2025). A Decade of Thunderstorm Patterns: A Comparative Study of Iraq and Russia. *Iraqi Journal of Science*, *66*(7), 3018-3027. https://doi.org/10.24996/ijs.2025.66.7.28

Al-khulaifawi, I. A. J., & Ioshpa, A. R. (2025). Spatial and temporal assessment of thunderstorm frequency and their impacts on PM2.5 over Iraq. *Multidisciplinary Materials Chronicle*, 112–125. https://doi.org/10.62184/mmc.jmmc1100202531

Al-Khulaifawi, Imad & Ioshpa, Alexander. (2026). Spatial and Temporal Evaluation of the Frequency of Thunderstorms and their Effects on PM2.5 Distribution over Baghdad and Basra Airdromes. *Iraqi Journal of Environmental Sciences*. 2. 22-35. DOI:10.23851/ijes.v2i1.21

Al-Khulaifawi, I., & Mutar, A. (2026). Thundercloud assessment for the years 1990–2019 over the Baghdad airport station. *Theoretical and Applied Climatology*. https://doi.org/10.21203/rs.3.rs-8683928/v1

Al-Qadi, T. A., Muslih, K. D., & Shiltagh, A. G. (2021). Analysis of correlation and coupling between El Niño-Southern Oscillation and dust storms in Iraq from 1971 to 2016. *Iraqi Geological Journal*, *54*(1E), 103–113.https://doi.org/10. 46717/ igj.54. 1E.9Ms-2021-05-30

Arora, K., Ray, K., Ram, S., & Mehajan, R. (2023). The role of instability indices in forecasting thunderstorm and non-thunderstorm days across six cities in India. *Climate,* 11, 14. https://doi.org/10.3390/cli11010014

Asfur, Mustafa & Price, Colin & Yair, Yoav & Silverman, Jacob. (2023). Spatial variability of lightning intensity over the Mediterranean Sea correlates with seawater properties. *Sci Rep,* 13(1), 5834. https://doi.org/10.1038/s41598-023-33115-0

Atheeb, Z. A. . (2025). The Impact of Air Pollution in Iraq on the Environment: A Chemical Study of the Relationships between Pollutants and Climatic Conditions. *Central Asian Journal of Theoretical and Applied Science*, *6*(3), 427–439. https://doi.org/10.51699/cajotas.v6i3.1572

Augstein, E., H. Schimdt, and F. Ostapoff. (1974). The vertical structure of atmospheric planetary boundary layer in the undisturbed trade winds over the Atlantic Ocean, *Boundary Layer Meteorol*., 6, 129–150, doi:10.1007/BF00232480

Bennett, L. J., Browning, K. A., Blyth, A. M., Parker, D. J., & Clark, P. A. (2006). A review of the initiation of precipitating convection in the United Kingdom. *Quarterly Journal of the Royal Meteorological Society, 132*, 1001–1020. https://doi.org/10.1256/qj.05.54

Bentley, M., Gerken, T., Duan, Z., et al. (2024). Toward untangling thunderstorm-aerosol relationships: An observational study of regions centered on Washington, DC and Kansas City, MO. Atmospheric Research, 304, 107402. https://doi.org/10.1016/j.atmosres.2024.107402

Brázdil, R., Chromá, K., Púčik, T., et al. (2020). The climatology of significant tornadoes in the Czech Republic. *Atmosphere*, 11(7). 10.3390/atmos11070689

Buchard, V., Randles, C. A., da Silva, A. M., et al. (2017). The MERRA-2 aerosol reanalysis, 1980 onward. Part II: Evaluation and case studies. Journal of Climate, 30(17), 6851–6872. https://doi.org/10.1175/JCLI-D-16-0613.1

Chai, Tianfeng & Draxler, R.R. (2014). Root mean square error (RMSE) or mean absolute error (MAE)—Arguments against avoiding RMSE in the literature. *Geoscientific Model Development*. 7(3): 1247-1250. DOI:10.5194/gmd-7-1247-2014

Chen, D., & Chen, H.W. (2013). Using the Köppen classification to quantify climate variation and change: An example for 1901–2010. *Environmental Development*, 6(1), 69-79. Doi:10.1016/j.envdev.2013.03.007

Colarco, P., da Silva, A., Chin, M., & Diehl, T. (2010). Online simulations of global aerosol distributions in the NASA GEOS-4 model and comparisons to satellite and ground-based aerosol optical depth. *Journal of Geophysical Research: Atmospheres*, 115(D20). https://doi.org/10.1029/2009JD012820

Eiras-Barca, Jorge & Dominguez, Francina & Hu, Huancui & Garaboa Paz, Daniel & Miguez-Macho, Gonzalo. (2017). Evaluation of the moisture sources in two extreme landfalling atmospheric river events using an Eulerian WRF tracers tool. *Earth System Dynamics*. 8(4). 1247-1261. Doi:10.5194/esd-8-1247-2017

Emanuel, K. A. (1994). Atmospheric Convection, Oxford Univ. Press, New York.

EPA (2018). Technical assistance document for the reporting of daily air quality: The AirQuality Index (AQI), September 2018 [edition]. U.S. Environmental Protection Agency, Office of Air Quality Planning and Standards, Air Quality Assessment Division, Research Triangle Park,NC, USA

*(PDF) PM2.5 Forecast System by Using Machine Learning and WRF Model, A Case Study: Ho Chi Minh City, Vietnam*. Available from: https://www.researchgate.net/publication/355885038_PM25_Forecast_System_by_Using_Machine_Learning_and_WRF_Model_A_Case_Study_Ho_Chi_Minh_City_Vietnam

Galindo, N., Varea, M., Gil-Moltó, J., Yubero, E., & Nicolás, J. (2011). The influence of meteorology on particulate matter concentrations at an urban Mediterranean location. Water, Air, and Soil Pollution, 215(1), 365–372. https://doi.org/10.1007/s11270-010-0484-z

Gettelman, A., D. J. Seidel, M. C. Wheeler, and R. J. Ross. (2002). Multidecadal trends in tropical convective available potential energy, *Journal of Geophysical Research: Atmospheres, 107(D21),* 4606, Doi:10.1029/2001jd001082, 2002

Gupta, P., & Sayeed, A. (2024). MERRA2_CNN_HAQAST bias corrected global hourly surface total PM2.5 mass concentration, V1. Goddard Earth Sciences Data and Information Services Center (GES DISC). https://doi.org/10.5067/OCKK5HCFW5N3

Kalnay E, Kanamitsu M, Kistler R, Collins W, Deaven D, Gandin L, Iredell M, Saha S, White G, Woollen J, Zhu Y, Chelliah M, Ebisuzaki W, Higgins W, Janowiak J, Mo KC, Ropelewski C, Wang J, Leetmaa A, Reynolds R, Jenne R, Joseph D. (1996). The NCEP/NCAR 40-year reanalysis project. Bull Am Meteorol Soc 77(3):437–470. https://psl.noaa.gov

Kolendowicz, L., Taszarek, M., & Czernecki, B. (2017). Atmospheric circulation and sounding-derived parameters associated with thunderstorm occurrence in Central Europe. *Atmospheric Research*, 191, 101–114. https://doi.org/10.1016/j.atmosres.2017.03.009

Krider, E. P. (2021). "Thunderstorm". *Encyclopedia Britannica*. Retrieved 14 January 2021. https://www.britannica.com/science/thunderstorm

Kunz, M., Wandel, J., Fluck, E., Baumstark, S., Mohr, S., & Schemm, S. (2020). Ambient conditions prevailing during hail events in central Europe. *Natural Hazards and Earth Systems Sciences, 20*, 1867–1887. https://doi.org/10.5194/nhess-20-1867-2020

Liou, K. N., & Ou, S. C. (1989). The role of cloud microphysical processes in climate: An assessment from a one-dimensional perspective. *Journal of Geophysical Research: Atmospheres*, 94, 8599–8607. Doi: 10.1029/JD094iD06p08599

Misva. (2021). *Precipitable Water (PW)*. MISVA – Méthode d'Analyse Intégrée pour la Prévision du Temps en Afrique de l'Ouest. https://misva.aeris-data.fr/en/precipitable-water-pw/

Mohammed, I. I., & Hassoon, A. F. . (2019). Effect of Rainfall Quantity on the Frequency of Severe Dust Storm in Iraq. *Basrah Journal of Agricultural Sciences,* 32, 156–170. https://doi.org/10.37077/25200860.2019.265

Mutar, A. G. (2024). The effect of atmospheric organic carbon on precipitation formation in southern Iraq: Case study. *Journal of Education for Pure Science- University of Thi-Qar*, *14*(3), 1–11. https://doi.org/10.32792/jeps.v14i3.537

Pekárová, P., Mészáros, J., Miklánek, P., et al. (2021). Post-flood field investigation of the June 2020 flash flood in the upper Muráň River basin and the catastrophic flash flood scenario. *Journal of Hydrology and Hydromechanics*. https://doi.org/10.2478/johh-2021-0015

Púčik, T., Valachová, M., & Zacharov, P. (2013). Upper tropospheric conditions in relation to the cloud top features of 15 August 2010 convective storms. *Atmospheric Research*, 123, 249–267. https://doi.org/10.1016/j.atmosres.2012.10.006

Roostaei, V., Abbasi, A., Gharibzadeh, F., Faridi, S., Naddafi, K., Yunesian, M., Hassanvand, M.S. (2024). Vertical Distribution of Air Particulate Matter ($PM_1$, $PM_{2.5}$, and $PM_{10}$) in Different Regions of Tehran. Aerosol Air Qual. Res. 24, 240036. https://doi.org/10.4209/aaqr.240036

Roy, P., Rao, T. N., Biswasharma, R., et al. (2023). Space–time variation of large hail-producing mesoscale convective systems over a complex terrain of the Indian subcontinent. *International Journal of Climatology*, 43(6), 3023–3039. https://doi.org/10.1002/joc.8015

Sadar, M. W., Al-Jiboori, H. M., & Al-Timimi, K. Y. (2023). Spatial analysis of PM2.5 concentration over Iraq during 2003–2020. *Journal of the Earth and Space Physics*, 48(4), 173–182. http://doi.org/10.22059/jesphys.2022.344671.1007441

Sae-Jung, J., Bentley, M., Gerken, T. & Duan, Z. (2025). The Impact of Urban Particulate Matter on Lightning Frequency in Thunderstorms: A Case Study of the Bangkok Metropolitan Region. *Earth Syst Environ* 9(4), 3137–3153. DOI:10.1007/s41748-024-00474-1

Shukur, Z. K. J. (2025). Analysis of the Spatial and Temporal Variability of Thunderstorms and Their General Trend in Iraq. Journal of Social Sciences and Humanities Research Fundamentals. 5(4): 157-174. DOI:10.55640/jsshrf-05-04-27

Sirikaew, S., Wichapeng, S., Wipawattanti, P., & Kangwanwit, W. . (2025). Atmospheric Precipitable Water Estimation from Long-Term Ground-Based Meteorological Data Using an Artificial Neural Network Model. *Burapha Science Journal*, *30*(3 September-December), 866–883. retrieved from https://li05.tci-thaijo.org/index.php/buuscij/article/view/716

Steiger, S. M., & Orville, R. E. (2003). Cloud-to-ground lightning enhancement over Southern Louisiana. *Geophysical Research Letters*, 30(20), 1–4. https://doi.org/10.1029/2003GL017923

Stull, R. (2017). Practical meteorology: An algebra-based survey of atmospheric science. Vancouver, BC, Canada.

Sun, M., Qie, X., Mansell, E. R., et al. (2023). Aerosol impacts on storm electrification and lightning discharges under different thermodynamic environments. *Journal of Geophysical Research: Atmospheres*, 128(1), e2022JD037450. https://doi.org/10.1029/2022JD037450

Taszarek, M., Allen, J. T., Groenemeijer, P., et al. (2020). Severe convective storms across Europe and the United States. *Journal of Climate*, 33, 10239–10261. https://doi.org/10.1175/JCLI-D-20-0345.1

Trapp, R. J. (2013). Mesoscale-convective processes in the atmosphere. Cambridge University Press. https://doi.org/10.1017/CBO9781139047241

Twomey, S. (1977). Influence of pollution on the shortwave albedo of clouds. *Journal of the Atmospheric Sciences*, 34(7), 1149–1152. Doi:10.1175/1520-0469

Wang, Z., Chai, H., Ming, L., Ye, Y., Ma, H., & Chen, P. (2025). Estimation of PM2.5 concentration in southern China using stacked machine learning models based on GNSS and radiosonde precipitable water vapor. *Advances in Space Research*, *76*(3), 1338–1355. Doi:10.1016/j.asr.2025.05.038